Spectrum lines of Kr XXVIII–Kr XXXIV observed in the JET tokamak

B. Denne, E. Hinnov,* J. Ramette,† and B. Saoutic‡
JET Joint Undertaking, Abingdon, Oxon OX14 3EA, United Kingdom
(Received 28 November 1988)

Spectra of highly ionized krypton in the wavelength range 40–335 Å have been observed in the Joint European Torus tokamak plasmas, into which small amounts of Kr were admitted. Among the observed lines are all the strong resonance lines within the $n=2$ shell from fluorinelike to lithiumlike krypton, as well as all the stronger magnetic dipole lines that are expected to occur in these spectra. The wavelengths of the krypton lines were determined using known wavelengths of lines of elements intrinsic in the plasma, mostly carbon and nickel lines, as standards. In most cases of stronger lines, the accuracy is estimated to ±0.025 Å, or better.

I. INTRODUCTION

In the large tokamaks of today, such as the Joint European Torus (JET) and the Tokamak Fusion Test Reactor (TFTR), central electron temperatures in the range 5–10 keV are readily attained with auxiliary heating. This has motivated a continuation towards higher-Z elements in the search for suitable transitions for the spectroscopic diagnostics of such plasmas, with particular emphasis on transitions within the $n=2$ shell, such as resonance lines and, even more so, the magnetic dipole transitions arising within the ground configurations (see Refs. 1 and 2 and references given therein). In the present experiment, the spectra of highly ionized krypton ($Z=36$), Kr XXVIII (fluorinelike)–Kr XXXIV (lithiumlike), have been studied. Of these, Kr XXVIII and Kr XXIX have been previously investigated by Wyart *et al.*[3] on the TFR tokamak, and Dietrich *et al.*[4] using a z-pinch plasma light source, while Kr XXXIII and Kr XXXIV have been observed in beam-foil spectra by Dietrich *et al.*[5] Semiempirical predictions of energy-level values and wavelengths for Li-like to F-like ions have been made by Edlén,[6–9] based on theoretical calculations by Cheng, Kim, and Desclaux.[10] These predictions aided the identification of the lines observed in the present work. Finally, Feldman *et al.*[11] have calculated line intensities for allowed and forbidden transitions for Be- to O-like ions (for unity abundance) under tokamak plasma conditions.

II. EXPERIMENT

A mixture of 2.4 vol% Kr in D_2 was admitted into 4–5 MA, ohmically heated, JET tokamak plasmas at a preselected time during the quasisteady phase of the discharge. The discharges were characterized by central electron temperatures in the range 3–4.2 keV and central electron densities of $(2.8–3.8)\times10^{13}$ cm^{-3}. A typical set of temperature and density radial profiles is shown in Fig.

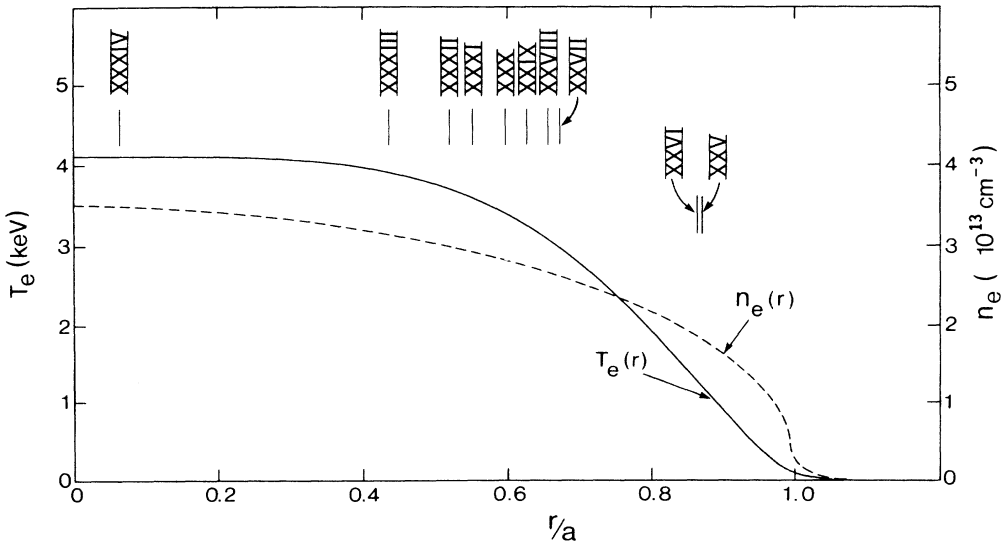

FIG. 1. Typical radial profiles of electron density and temperature. The approximate locations of the emission shells of several ionization stages of krypton are shown.

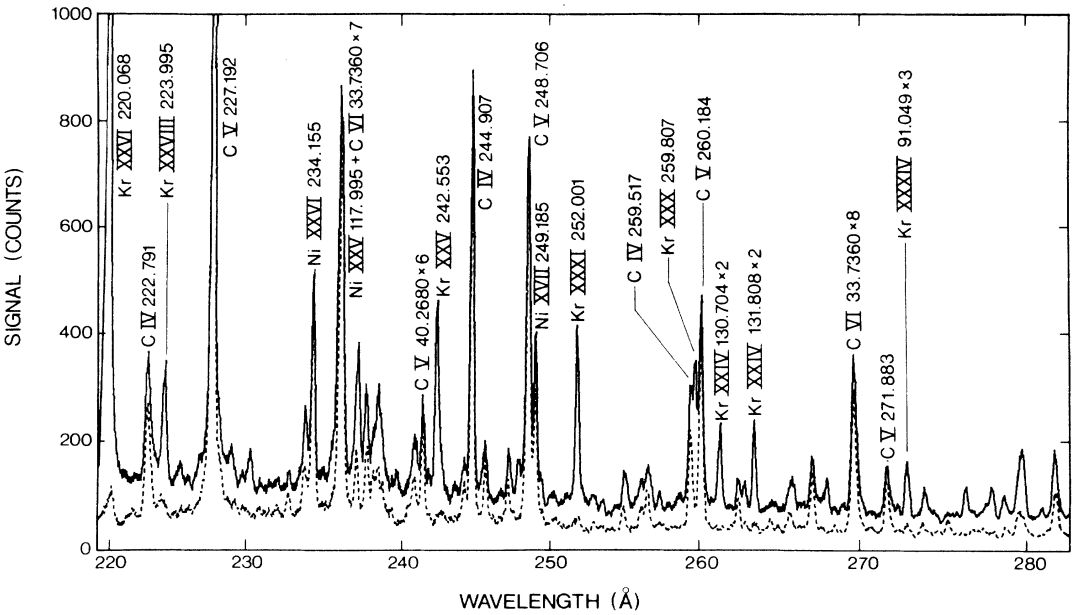

FIG. 2. Spectrum in the 220–280 Å range before (dashed line) and after the admission of Kr.

1, along with the approximate locations of the emission shells of several ionization stages of krypton, according to previous observation that the radial distribution of the emission from a given ion peaks at a radius at which the electron temperature is equal to the ionization potential of that ion. Spectra were recorded using a 2-m extreme grazing-incidence (Schwob-Fraenkel) spectrometer,[12] equipped with a 600-g/mm grating and two microchannel-plate image intensifier-converter detector systems, fiber-optically coupled to 1024-element photodiode arrays. The two detectors are movable along the Rowland circle, and cover 20–60-Å sections of spectra, depending on wavelength. The spectral resolution [full width at half maximum (FWHM)] is approximately 0.2 Å. The spectral range covered was 40–335 Å, for which five discharges were needed. An example spectrum before and after the krypton was introduced is shown in Fig. 2. The wavelengths of the krypton lines were determined using known wavelengths of lines of elements intrinsic in the plasma, mostly C IV, C V, C VI, and nickel lines of various ionization stages, as standards.[13–15] Oxygen lines[13,16] were used to a lesser extent, due to the low oxygen content of the plasmas. The differences between the measured and tabulated wavelengths for the standards were fitted, as a function of wavelength, using a weighted least-squares fitting program, utilizing orthogonal (Chebyshev) polynomials up to sixth order, in order to obtain a calibration curve. The wavelengths of the measured krypton lines were then determined by interpolation. Wavelengths of the stronger Kr lines, thus obtained, were then used as secondary standards.

III. EXCITATION CONDITIONS

The principal endeavor of this paper is the measurement of wavelengths, but we shall attempt to say something about the relative intensities of the observed lines. This latter task is only semiquantitative, because the observations are based on five different discharges, which varied somewhat in temperature and density as well as in the total amount of injected krypton. Furthermore, the relative sensitivity of the instrument at different wavelengths is *a priori* only vaguely known. Nevertheless some features of the spectra characteristic of tokamak discharges are evident in the observations.

As seen from Fig. 1, all the ionization stages of krypton under discussion are essentially at the same electron density, $n_e \approx 3 \times 10^{13}$ cm^{-3}, and at temperatures that are much higher than the excitation potential of the lines to be discussed, which is typically less than 200 eV. This means that practically every electron collision is capable of exciting the ion, and at the prevailing density the higher collisional transition rates are typically $\leq 10^4$ sec^{-1}, i.e., much lower than the radiative transition rates. Consequently, only the ground levels in the various ionization stages are appreciably populated, and only such lines that originate from upper levels connected to the ground levels by transitions with high line strengths or f values are expected to be strong. Although it is possible for some atoms in high ionization stages to drift outwards to regions of lower temperature and higher neutral deuterium density where they may recombine and emit radiation from highly excited states, such processes are relatively insignificant in ohmically heated plasmas.

We have, therefore, a situation in which all the ionization stages of krypton, from XXVIII to XXXIII, are present in roughly comparable amounts, and disappear on a time scale determined by the ion confinement time, and are subject to excitation essentially by single electron collisions from the respective ground levels. In the situation depicted in Fig. 1, the status of Kr XXXIV is somewhat marginal—the density of this ion may still be substantial-

ly lower than for the other ions at the prevailing electron temperature.

There are three levels that require special consideration: the $2s^2 2p^4\,{}^3P_0$ level in Kr XXIX, the $2s2p\,{}^3P_0$ in Kr XXXIII, and the $2s^2 2p^2\,{}^3P_2$ level in Kr XXXI have sufficiently long radiative lifetimes that their decay may not be regarded as instantaneous relative to collisional transitions. Of these, the $^3P_0$ probably do not affect appreciably the spectra—thus in Kr XXIX it probably only changes slightly the $2s2p^5\,{}^3P_1$ excitation rate, and in Kr XXXIII, where the $^3P_0$ is a true metastable state, it is likely to decay preferentially by collisional transitions to the nearby $2s2p\,{}^3P_1$ level and from there radiatively to the ground level. The $2s^2 2p^2\,{}^3P_2$ level in Kr XXXI is only marginally metastable at the prevailing electron density, but its effect is nevertheless noticeable on the population of excited states of higher J.

IV. RESULTS

The wavelengths of all observed lines of Kr XXVIII–Kr XXXIV are given in Table I, along with their classifications. For comparison, the semiempirically predicted wavelengths by Edlén[6–9] are also given.

TABLE I. Observed lines of Kr XXVIII–Kr XXXIV. w, weak line; t, tentative identification; bl, blended.

Observed wavelength (Å)	Spectrum	Classification	Comment	Predicted wavelength[a] (Å)
52.594±0.02	XXVIII	$2s^2 2p^5\,{}^2P_{3/2}-2s2p^6\,{}^2S_{1/2}$		52.589
53.640±0.03	XXIX	$2s^2 2p^4\,{}^3P_2-2s2p^5\,{}^3P_1$		53.631
54.596±0.05	XXX	$2s^2 2p^3\,{}^2D_{5/2}-2s2p^4\,{}^2P_{3/2}$	w	54.636
56.976±0.05	XXXI	$2s^2 2p^2\,{}^3P_1-2s2p^3\,{}^3S_1$	t	57.035
58.700±0.05	XXIX	$2s^2 2p^4\,{}^3P_0-2s2p^5\,{}^3P_1$		58.734
59.714±0.03	XXIX	$2s^2 2p^4\,{}^3P_2-2s2p^5\,{}^3P_2$	bl Kr XXXI	59.689
59.748±0.03	XXXI	$2s^2 2p^2\,{}^3P_2-2s2p^3\,{}^3S_1$	bl Kr XXIX	59.813
60.332±0.03	XXX	$2s^2 2p^3\,{}^4S_{3/2}-2s2p^4\,{}^4P_{1/2}$		60.255
60.732±0.025	XXX	$2s^2 2p^3\,{}^4S_{3/2}-2s2p^4\,{}^4P_{3/2}$		60.570
62.411±0.05	XXXI	$2s^2 2p^2\,{}^3P_1-2s2p^3\,{}^3P_1$		62.378
63.103±0.025	XXXI	$2s^2 2p^2\,{}^3P_2-2s2p^3\,{}^3P_2$		63.071
63.671±0.03	XXX	$2s^2 2p^3\,{}^2D_{3/2}-2s2p^4\,{}^2D_{3/2}$	w	63.772
64.65 ±0.10	XXXII	$2s^2 2p\,{}^2P_{3/2}-2s2p^2\,{}^2P_{3/2}$	t	64.59
		$2s^2 2p\,{}^2P_{3/2}-2s2p^2\,{}^2P_{1/2}$	t	65.0
65.352±0.02	XXXI	$2s^2 2p^2\,{}^3P_0-2s2p^3\,{}^3D_1$		65.371
66.538±0.025	XXXII	$2s^2 2p\,{}^2P_{1/2}-2s2p^2\,{}^2S_{1/2}$		66.6
68.733±0.03	XXVIII	$2s^2 2p^5\,{}^2P_{1/2}-2s2p^6\,{}^2S_{1/2}$		68.728
69.414±0.033	XXIX	$2s^2 2p^4\,{}^3P_1-2s2p^5\,{}^3P_1$		69.412
69.957±0.02	XXXII	$2s^2 2p\,{}^2P_{1/2}-2s2p^2\,{}^2D_{3/2}$		69.83
71.875±0.025	XXX	$2s^2 2p^3\,{}^4S_{3/2}-2s2p^4\,{}^4P_{5/2}$		71.886
72.756±0.020	XXXIII	$2s^2\,{}^1S_0-2s2p\,{}^1P_1$		72.65
74.663±0.05	XXIX	$2s^2 2p^4\,{}^1D_2-2s2p^5\,{}^3P_1$		74.653
76.610±0.035	XXXI	$2s^2 2p^2\,{}^3P_2-2s2p^3\,{}^3D_3$		76.517
79.557±0.05	XXXI	$2s^2 2p^2\,{}^3P_1-2s2p^3\,{}^3D_2$		79.652
79.947±0.03	XXIX	$2s^2 2p^4\,{}^3P_1-2s2p^5\,{}^3P_2$		79.909
84.94 ±0.10	XXXII	$2s^2 2p\,{}^2P_{3/2}-2s2p^2\,{}^2D_{5/2}$	w,t	84.37
86.26 ±0.05	XXX	$2s^2 2p^3\,{}^2D_{5/2}-2s2p^4\,{}^4P_{3/2}$	w	85.948
86.98 ±0.04	XXIX	$2s^2 2p^4\,{}^1D_2-2s2p^5\,{}^3P_2$		86.935
91.049±0.025	XXXIV	$2s\,{}^2S_{1/2}-2p\,{}^2P_{3/2}$		91.00
95.057±0.05	XXXI	$2s^2 2p^2\,{}^3P_2-2s2p^3\,{}^3D_1$		95.108
110.62 ±0.06	XXX	$2s^2 2p^3\,{}^2D_{5/2}-2s2p^4\,{}^4P_{5/2}$	w	110.67
160.90 ±0.10	XXX	$2s^2 2p^3({}^4S_{3/2}-{}^2P_{1/2})$	t,bl C V	160.8
169.845±0.025	XXXIII	$2s^2\,{}^1S_0-2s2p\,{}^3P_1$		170.11
174.036±0.026	XXXIV	$2s\,{}^2S_{1/2}-2p\,{}^2P_{1/2}$		173.87
190.515±0.03	XXIX	$2s^2 2p^4({}^3P_2-{}^1D_2)$		190.45
203.021±0.02	XXXII	$2s^2 2p({}^2P_{1/2}-{}^2P_{3/2})$		203.01
205.247±0.025	XXX	$2s^2 2p^3({}^4S_{3/2}-{}^2D_{5/2})$		205.1
223.995±0.03	XXVIII	$2s^2 2p^5({}^2P_{3/2}-{}^2P_{1/2})$		223.95
235.48 ±0.05	XXXIII	$2s2p({}^3P_1-{}^3P_2)$	w,bl	235.1
235.95 ±0.10	XXIX	$2s^2 2p^4({}^3P_2-{}^3P_1)$	bl Ni XXV, C VI	235.89
252.001±0.02	XXXI	$2s^2 2p^2({}^3P_0-{}^3P_1)$		251.97
259.807±0.02	XXX	$2s^2 2p^3({}^4S_{3/2}-{}^2D_{3/2})$		259.7

[a]Edlén, Refs. 6–9.

TABLE II. Energy levels of Kr XXVIII–Kr XXXIV.

Configuration	Level	Energy (cm^{-1}) Present experiment	Previous experiment		Semiempirical prediction[d]
Kr XXVIII					
$2s^2 2p^5$	$^2P_{3/2}$	0	0[a]	0[b]	0
	$^2P_{1/2}$	446 440±60	446 800	446 600±500	446 352
$2s2p^6$	$^2S_{1/2}$	1 901 340±640	1 901 700	1 901 140±800	1 901 358
Kr XXIX					
$2s^2 2p^4$	$^3P_2$	0	0[a]	0[b]	0
	$^3P_0$	160 780±1600		160 400±750	162 011
	$^3P_1$	423 820±180		424 600±520	423 933
	$^1D_2$	524 890±80	$525\,066+x$		525 066
$2s2p^5$	$^3P_2$	1 674 625±500	1 675 500	1 674 170±840	1 675 351
	$^3P_1$	1 864 360±700	1 865 300	1 864 280±810	1 864 603
Kr XXX					
$2s^2 2p^3$	$^4S_{3/2}$	0			0
	$^2D_{3/2}$	384 900±30			385 111
	$^2D_{5/2}$	487 220±60			487 493
	$^2P_{1/2}$	621 500±380			621 813
$2s2p^4$	$^4P_{5/2}$	1 391 300±480			1 391 091
	$^4P_{3/2}$	1 646 580±680			1 650 982
	$^4P_{1/2}$	1 657 500±820			1 659 606
	$^2D_{3/2}$	1 955 480±740			1 953 195
	$^2P_{3/2}$	2 318 860±1700			2 317 795
Kr XXXI					
$2s^2 2p^2$	$^3P_0$	0			0
	$^3P_1$	396 820±30			396 865
	$^3P_2$	478 180±300			478 296
$2s2p^3$	$^3D_1$	1 530 180±470			1 529 733
	$^3D_2$	1 653 780±790			1 652 332
	$^3D_3$	1 783 490±670			1 785 198
	$^3P_1$	1 999 110±1300			1 999 996
	$^3P_2$	2 062 890±700			2 063 817
	$^3S_1$	2 151 950±1500			2 150 179
Kr XXXII					
$2s^2 2p$	$^2P_{1/2}$	0			0
	$^2P_{3/2}$	492 560±50			492 596
$2s2p^2$	$^2D_{3/2}$	1 429 450±410			1 432 115
	$^2D_{5/2}$	1 669 860±1400			1 677 804
	$^2S_{1/2}$	1 502 900±570			1 502 292
	$^2P_{3/2}$	2 039 350±2400			2 040 784
Kr XXXIII					
$2s^2$	$^1S_0$	0		0[c]	0
$2s2p$	$^3P_1$	588 770±90		588 580±1700	587 844
	$^3P_2$	1 013 440±130			1 013 260
	$^1P_1$	1 374 457±380			1 376 480
Kr XXXIV					
$2s$	$^2S_{1/2}$	0		0[c]	0
$2p$	$^2P_{1/2}$	574 594±90		574 220±860	575 137
	$^2P_{3/2}$	1 098 310±300		1 097 940±1200	1 098 849

[a]Wyart *et al.* (Ref. 3).
[b]Dietrich *et al.* (Ref. 4).
[c]Dietrich *et al.* (Ref. 5).
[d]Edlén (Refs. 6–9).

The results for the individual ions are discussed below. The energy-level values derived from the measured wavelengths are summarized in Table II.

Kr XXVIII–F sequence

In this sequence we expect to observe three lines: two resonance lines from the $2s2p^6\,^2S_{1/2}$ level to the ground configuration $2s^22p^5\,^2P_{3/2,1/2}$ and one magnetic dipole ($M1$) transition between the ^2P levels of the ground configuration. The observed wavelengths for these lines are 52.594±0.02–68.733±0.03 Å and 223.995±0.03 Å, respectively. The first one of these is close to the 1–5 transition of C VI in second grating order, and has been measured relative to this line. The measured resonance line wavelengths are in good agreement with previous measurements (Table II) as well as with the semiempirical predictions of Edlén.[6] For the $M1$ line, there is good agreement both with the semiempirical predictions by Edlén[6] and Curtis and Ramanujam[17] and the calculated value of Kim and Huang[18] within the mutual error limits.

As the intensity ratio of the resonance lines depends only on the radiative branching ratio from the $2s2p^6\,^2S_{1/2}$ level and the magnetic dipole line must be stronger than the 68.7-Å line, the measured intensity ratios offer an opportunity for checking the sensitivity of the spectrometer at different wavelengths.

The branching ratio of $(2s2p^6\,^2S_{1/2}\rightarrow 2s^22p^5\,^2P_{3/2})$: $(2s2p^6\,^2S_{1/2}\rightarrow 2s^22p^5\,^2P_{1/2})$ is 4.6 according to Cheng *et al.*[10] Our measured intensity ratio I(52 Å)/I(68 Å) is only ~2.2, indicating a rather substantial drop in sensitivity towards the shorter wavelength.

The rate of emission for the 224-Å line, we calculate as approximately 1.7 times that of the 68.7-Å line, in fair agreement with the measured value of ~1.6, even though this involves a different detector and a substantial wavelength difference.

Kr XXIX–O sequence

The relevant energy levels and observed lines are shown in Fig. 3. This ionization stage exhibits one of the exceptional cases of metastable levels above the ground level at tokamak densities—the $^3P_0$ level can only decay by an electric quadrupole transition, and has a calculated[19] transition rate of 6.5 sec^{-1}, which is low compared to collisional rates. We therefore expect this level to be approximately in Boltzmann equilibrium with the ground level.

This in itself would not be a drawback, as it would affect only slightly the population of the $2s2p^5\,^3P_1$ level, but unfortunately for the detailed comparison of intensities many lines of this ionization stage are plagued by accidental blendings. Thus, the principal line, 59.714 Å, is blended by a transition in Kr XXXI at 59.748 Å. (The stated wavelengths have been obtained by comparing the observed line shape in second grating order in a discharge with substantially lower temperature, favoring the Kr XXIX line, with that of the first-order line shape.) The transition $2s^22p^4\,^1D_2$–$2s2p^5\,^1P_1$, which is expected to be weak because of a lack of a substantial population mechanism, overlaps with the 1–4 transition of C VI in second order. No change in the intensity of the carbon line is observed when the krypton is admitted. Thus no trace of this Kr XXIX line (nor any other singlet line of this ion) has been found, although both Wyart *et al.*[3] and Dietrich *et al.*[4] have observed it.

Therefore the $^3P_1$ and $^3P_2$ levels of the $2s2p^5$ configuration are the only observed electric-dipole-excited levels of Kr XXIX. Although each is observed by multiple transitions, most of them are too weak for adequate measurement of branching ratios.

In the ground configuration there are two observable magnetic dipole lines, but again one of them is severely blended by the combination of the berylliumlike nickel resonance line (117.995 Å) in second order, and the C VI resonance line (33.7360 Å) in seventh order. It is therefore not feasible to derive any usable intensity ratios for the two $M1$ lines. However, we can say that, to within a factor of 2, the 236- and 190-Å lines are of comparable intensity, with perhaps the 236-Å line the somewhat stronger of the two.

Besides these two lines, there are two other $M1$ lines which fall outside the wavelength range covered in the present experiment, but may be predicted from Ritz combinations: $^3P_1\rightarrow\,^3P_0$ at 380±2 Å, which is a line that

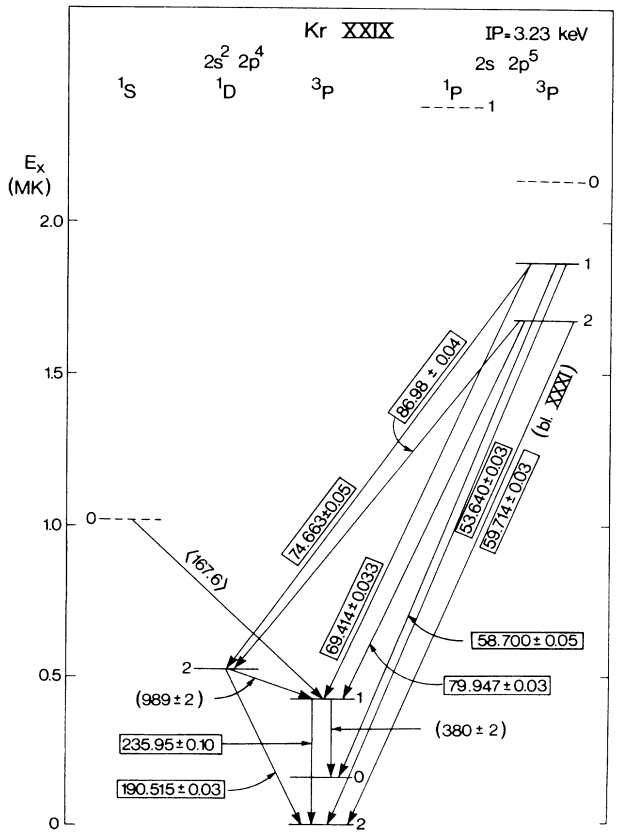

FIG. 3. Energy-level diagram of Kr XXIX. Wavelengths in boxes have been measured in the present work. The ionization potential (IP) is given at the top.

should be fairly strong ($\sim\frac{1}{8}$ of the 236-Å line[19]), and $^1D_2 \rightarrow {}^3P_1$ at 989±2 Å, expected to be considerably weaker because of the strong branching ratio against it.

Finally, there is the $^1S_0 \rightarrow {}^3P_1$ transition, predicted[6] to occur at 167.6 Å. This transition has been difficult to observe in tokamaks for any element, and the present experiment is no exception. Although it has a fairly substantial transition probability (to $^3P_1$), the excitation rate (from $^3P_2$) is evidently too minute for observation.

Kr XXX–N sequence

In the nitrogenlike Kr XXX (Fig. 4), there are three strong lines at short wavelengths corresponding to the $2s^2 2p^3\,{}^4S - 2s 2p^4\,{}^4P$ transitions, at 71.875±0.025, 60.732±0.025, and 60.332±0.03 Å, respectively. Their measured intensities are about in the ratio 85:100:28, to be compared to the calculated[11] ratio 57:100:34, again indicating a loss of response towards the shorter wavelengths at a rate approximately consistent with that noted in the case of Kr XXVIII.

In addition, three other, much weaker lines have been ascribed to originate from the three $J=\frac{3}{2}$ states of the $2s2p^4$ configuration and one from the $^4P_{5/2}$ level, at 110.62±0.06 Å. The other branch from $^4P_{5/2}$, to $^2D_{3/2}$, which should be considerably stronger, is hidden in a strong emission of Kr XX. The measured intensity ratio

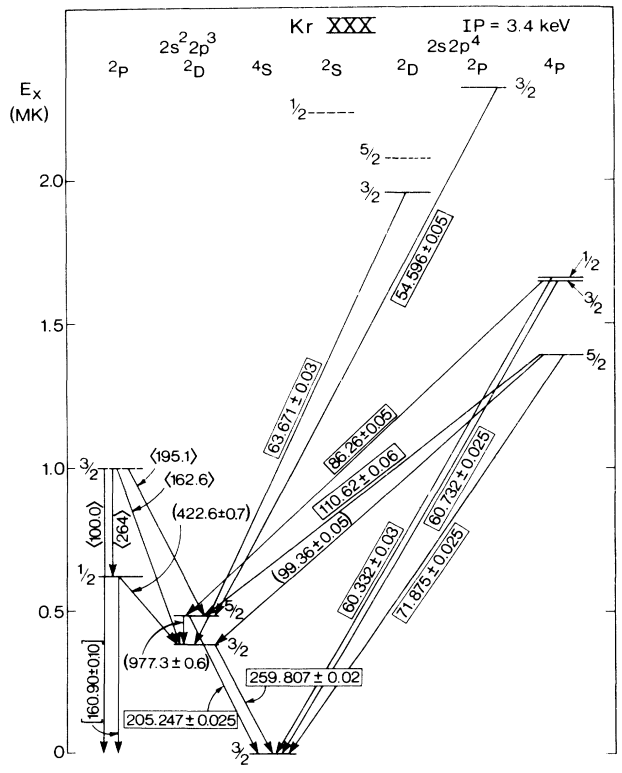

FIG. 4. Energy-level diagram of Kr XXX. For explanation of features, see Fig. 3 caption. Square brackets denote tentative identifications and angle brackets wavelengths predicted by Edlén.

of the (110.6:71.8)-Å lines is roughly 1:12, the same as expected from the branching ratio,[10] indicating approximately equal sensitivity at these wavelengths, whereas the ratio of the (86.2:60.7)-Å lines, with large uncertainty, seems to be about 1:23 compared to the expected 1:32. The sensitivity therefore appears to have a maximum around 75 Å for this detector, and decrease rapidly towards shorter wavelengths, and less rapidly towards longer wavelengths.

There is no trace of transitions from the $J=\frac{1}{2}$ or $\frac{5}{2}$ doublet levels of the $2s2p^4$ configuration, all of which have low collisional transition probabilities from the ground level.

Within the ground configuration we have observed the $2s^2 2p^3\,{}^4S_{3/2} - 2s^2 2p^3\,{}^2D_{3/2}$ $M1$ line at 259.807±0.02 Å, and $2s^2 2p^3\,{}^4S_{3/2} - 2s^2 2p^3\,{}^2D_{5/2}$ at 205.247±0.025 Å. The first one of these lies between the C V $1s2p\,{}^3P - 1s3s\,{}^3S$ feature at 260.184 Å and the C IV $1s^2 2p\,{}^2P - 1s^2 5d\,{}^2D$ transitions at 259.517 Å, while the second one is near high-order C V and C VI resonance lines. The measured wavelengths imply 102 320±65 cm^{-1} for the ^2D splitting, giving the wavelength 977.3±0.6 Å for the $^2D_{3/2}$-$^2D_{5/2}$ transition, which is uncomfortably close to the C III resonance line.

Besides these lines, we have observed a widening of the fourth order of the C V resonance line (161.072 Å) in a manner that would indicate the presence of a krypton line at about 160.90±0.10 Å, which we have tentatively assigned to the $2s^2 2p^3\,{}^4S_{3/2} - 2s^2 2p^3\,{}^2P_{1/2}$ transition. This allows the $^2D_{3/2} - {}^2P_{1/2}$ transition wavelength to be estimated from Ritz combinations: 422.6±0.7 Å.

Kr XXXI–C sequence

The Kr XXXI energy levels and observed lines are shown in Fig. 5. Only one of the short-wavelength lines, at 65.352 Å, is very strong, consistent with the expectation that only the ground level is appreciably populated. However, the $^3P_2$ level of the ground configuration has a radiative transition probability of only about 3.6×10^3 sec^{-1} (Cheng *et al.*[10] corrected for our estimated wavelength) which is not large enough so as to make collisional transitions entirely negligible. As a consequence, this level may also be somewhat populated, although well below the Boltzmann equilibrium value, but nevertheless sufficient to make some contribution to the collisional population of the higher-J triplet levels of the $2s2p^3$ configuration.

No lines connecting to the singlet levels or the $^5S_2$ level have been found. Of the measured lines, the $2s^2 2p^2\,{}^3P_2 - 2s2p^3\,{}^3S_1$ transition nearly overlaps with the strongest line of Kr XXIX. The composite line is, however, clearly wider than expected for a single line, and, as mentioned in the section on Kr XXIX, a measurement of the second-order line in a different discharge enabled the determination of the wavelength. (In third and fourth order the composite line is further blended—with the very strong Kr XXVI $3s\,{}^2S_{1/2} - 3p\,{}^2P_{3/2}$ resonance line and with the $2p$-$3d$ transitions of O IV, respectively.) The other transition from $2s2p^3\,{}^3S_1$, to $^3P_1$, is also blended in

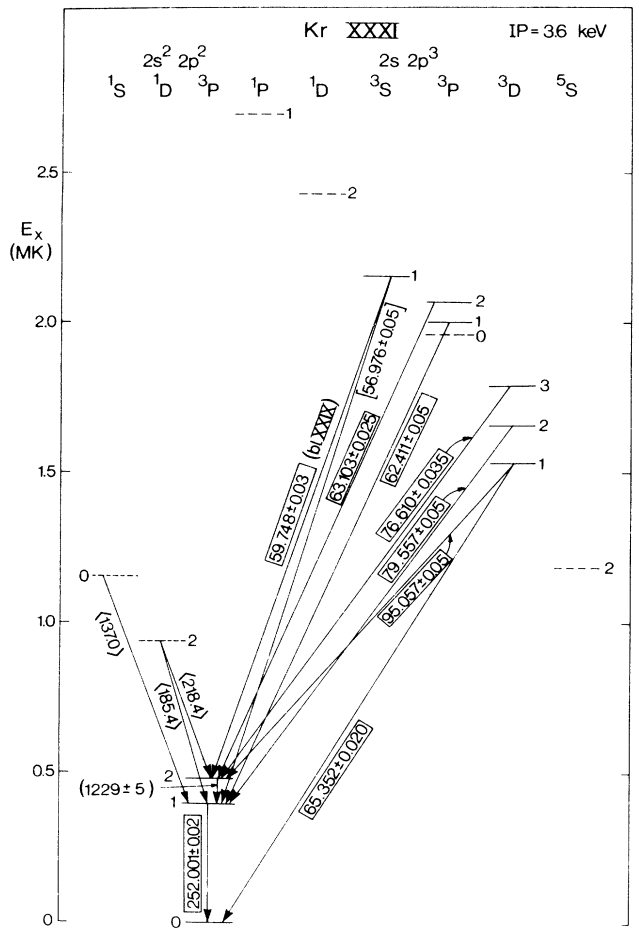

FIG. 5. Energy-level diagram of Kr XXXI. For explanation of features, see captions of Figs. 3 and 4.

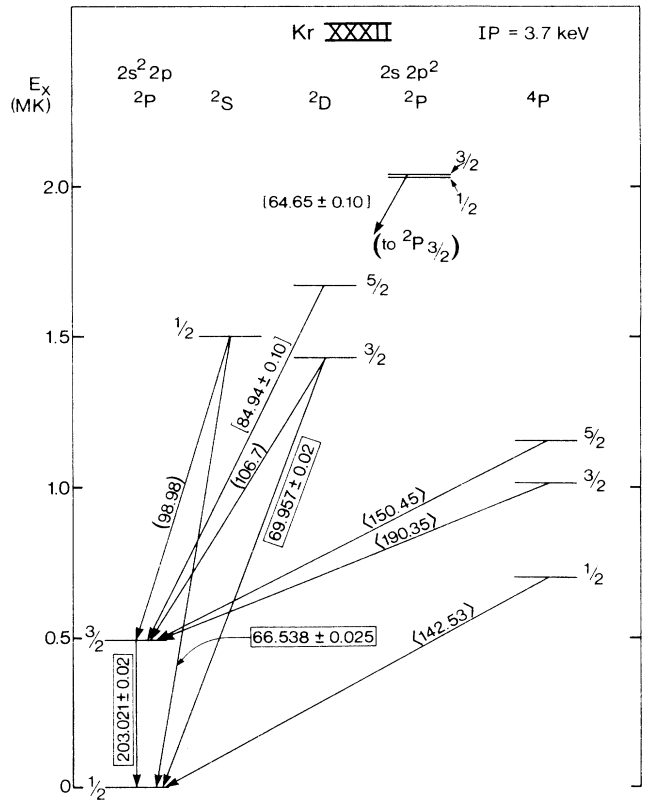

FIG. 6. Energy-level diagram of Kr XXXII. For explanation of features, see captions of Figs. 3 and 4.

first order with the 1–3 transition of C VI in second order. But in third order it is beginning to separate from the carbon line, and there we obtain the wavelength as 56.976±0.05 Å considered tentative because of the blending problems of the stronger component, $^3P_2$-$^3S_1$.

Within the ground configuration, the $^3P_1 \rightarrow {}^3P_0$ transition is strong and appears well isolated from other lines. Its wavelength is well determined by interpolation [principally between C IV (244.907 Å), Ni XVII (249.185 Å), and C V (260.184 Å)].

Most favorable for plasma diagnostic purposes would be the $^3P_2 \rightarrow {}^3P_1$ transition, because of its long wavelength. The wavelength of this line has been isoelectronically extrapolated (it is known up to Ge XXVII) as 1228 Å, in agreement with our value of 1229±5 Å, derived from Ritz combinations.

Kr XXXII – B sequence

There are two strong observed lines, 66.538 and 69.957 Å (Fig. 6), ascribed to this ionization stage. Of these, the 69-Å line is somewhat (~20%) stronger as would be expected from the f values to the $2s2p^2\,{}^2S_{1/2}$ and $^2D_{3/2}$ levels.

Besides these, there is a feature about 10 times weaker with a maximum at 64.65 Å, that appears to consist of two lines, which we consider to correspond to the $2s^2 2p\,{}^2P_{3/2} - 2s2p^2\,{}^2P_{3/2,1/2}$ transitions. If the two levels of the ground configuration, $2s^2 2p$, were comparably populated, these would be the strongest lines of the boronlike ion.

In addition, there is a weak line at 84.94 Å, which we have tentatively ascribed to the $2s^2 2p\,{}^2P_{3/2} - 2s2p^2\,{}^2D_{5/2}$ transition. The lines at 98.98 and 106.7 Å are from Ritz combinations.

There are several weak lines in the region around 142 Å that could be the intercombination line $2s^2 2p\,{}^2P_{1/2} - 2s2p^2\,{}^4P_{1/2}$. We suggest a line at 142.1 Å, but it is too uncertain for assignment.

Finally, there is the fairly strong $2s^2 2p\,{}^2P_{1/2} - 2s^2 2p\,{}^2P_{3/2}$ $M1$ transition at 203.021±0.02 Å. This line lies between the sixth-order C VI resonance line at 202.416 Å and the fifth-order C V intercombination line at 203.653 Å. Because of its favorable location and relatively long wavelength, this line is a prime candidate for high-temperature plasma diagnostics.

Kr XXXIII – Be sequence

The berylliumlike spectrum consists of two strong lines—the resonance line $2s^2\,{}^1S_0 - 2s2p\,{}^1P_1$, observed at 72.756±0.020 Å, and the intercombination line

$2s^2\,{}^1S_0-2s2p\,{}^3P_1$ at 169.845±0.025 Å. The resonance line was observed repeatedly, in first, second, third, and fourth order. However, in the even orders it overlaps with the Kr XXV $3s3p\,{}^1P_1-3s3d\,{}^1D_2$ transition. The wavelength given was thus derived from the first- and third-order observations only, and is in good agreement with a previously obtained value.[1]

The intercombination line was observed twice in first order. The measured wavelength agrees with a previous measurement[1] and also with a beam-foil observation by Dietrich *et al.*,[5] which, however, was much less accurate than the present measurement.

The intensity ratio of the resonance to intercombination line has been calculated by Feldman *et al.*[11] as 8.6:1, while a population calculation by Summers,[20] using collision strengths by Qian and Kim[21] gives 7.6:1. The experimentally obtained ratio is ~7:1, albeit with considerable uncertainty.

There is still another line, at 235.48±0.05 Å, in the flank of the second-order resonance line of Ni XXV. This line we have assigned to the magnetic dipole transition $2s2p\,{}^3P_1-2s2p\,{}^3P_2$. Although weak, it is quite definitely present, and the wavelength corresponds well with the value expected from isoelectronic extrapolations.[6,22]

Kr XXXIV – Li sequence

The $\frac{1}{2}$-$\frac{3}{2}$ transition in the lithiumlike ion was observed in first and third order, while in second order it overlaps with the C VI 2-3 transition at 182.1 Å. However, both the first and third order appear to be free of interfering lines, and the measurements are in good agreement with one another. The wavelength obtained, 91.049±0.025 Å, relies particularly on the third-order measurement, due to a lack of nearby good reference lines in first order. The value is slightly shorter than previously reported[1] (91.06 Å), the discrepancy being due, probably, to our different evaluation process.

The $\frac{1}{2}$-$\frac{1}{2}$ transition could only be observed in first order. It was seen on two shots in different detector positions. The wavelength obtained, 174.036±0.026 Å, relies mainly on the fifth-order C VI resonance line (168.680 Å) and the O V line at 172.169 Å. It is in good agreement with our previous result (174.03 Å).[1]

We have compared our measurements with the recent many-body perturbation-theory calculations by Johnson *et al.*[23] for the $2p$ fine structure and the $2s_{1/2}$-$2p_{1/2}$ splitting. The experimental values for krypton deviate from theory in a manner consistent with that observed for lower-Z members of the sequence. Johnson *et al.*[23] have shown this systematic difference to be of the order of the one-electron Lamb shift, however with clear deviations which they attribute to screening of the Lamb shift.

The intensities of the two lines appear somewhat low, compared to lines of earlier stages of ionization. Although the comparison of intensities of lines in different spectral regions—that involves different shots and different detectors—is somewhat precarious, we have a fairly good comparison of the 174-Å line intensity with that of the Be-like intercombination line (169.8 Å). If the number of ions along the line of sight were the same for Kr XXXIII and Kr XXXIV, we should expect roughly an intensity ratio of 2.5:1 in favor of the 174-Å line, whereas the observed ratio was about 0.65:1, in one shot, and about 1:1 in the following shot, in qualitative agreement with the observed shot-to-shot rise of electron temperature. This would also mean that at higher temperature there would be a considerable rise in the lithiumlike line intensities, and consequently, their applicability to plasma diagnostics would improve.

ACKNOWLEDGMENTS

The authors wish to thank the JET operating team for their cooperation and support during this experiment, in particular, Dr. C. Gowers, Dr. P. Lomas, Dr. A. Tanga and Dr. P. Thomas. Thanks are further due to Dr. H. P. Summers for his population calculations for Be-like Kr, to Dr. K. D. Lawson for generously communicating his nickel wavelengths prior to publication, and to Mr. H. S. Jensen for preparing the Kr-D_2 mixture. E.H. would like to thank the JET management and team for the hospitality he enjoyed during his visit under the Large Tokamak Tripartite Agreement.

*Permanent address: Princeton Plasma Physics Laboratory, Princeton, NJ 08543.

†Present address: Direction de la planification et de l'Evaluation des Programmes-Service Evaluation, Commissariat à l'Energie Atomique, 31-33 Rue de la Fédération, F-75752 Paris CEDEX 15, France.

‡Present address: Association EURATOM–Commissariat à l'Energie Atomique sur la Fusion, Centre d'Etudes Nucléaires–Cadarache, F-13108 St. Paul lez Durance, France.

[1]B. Denne and E. Hinnov, Phys. Scr. **35**, 811 (1987).

[2]E. Hinnov (unpublished).

[3]J. F. Wyart and TFR Group, Phys. Scr. **31**, 539 (1985).

[4]D. D. Dietrich, R. E. Stewart, R. J. Fortner, and R. J. Dukart, Phys. Rev. A **34**, 1912 (1986).

[5]D. D. Dietrich, J. A. Leavitt, H. Gould, and R. Marrus, Phys. Rev. A **22**, 1109 (1980).

[6]B. Edlén, Phys. Scr. **28**, 51 (1983).

[7]B. Edlén, Phys. Scr. **28**, 483 (1983).

[8]B. Edlén, Phys. Scr. **30**, 135 (1984).

[9]B. Edlén, Phys. Scr. **31**, 345 (1985).

[10]K. T. Cheng, Y.-K. Kim, and J. P. Desclaux, At. Data Nucl. Data Tables **24**, 111 (1979).

[11]U. Feldman, J. F. Seely, and A. K. Bhatia, At. Data Nucl. Data Tables **32**, 305 (1985).

[12]J.-L. Schwob, A. W. Wouters, S. Suckewer, and M. Finkenthal, Rev. Sci. Instrum. **58**, 1601 (1987).

[13]R. L. Kelly, J. Phys. Chem. Ref. Data **16**, Suppl. 1 (1987).
[14]C. Corliss and J. Sugar, J. Phys. Chem. Ref. Data **10**, 197 (1981).
[15]K. D. Lawson (private communication).
[16]B. Edlén, Phys. Scr. **11**, 366 (1975).
[17]L. J. Curtis and P. S. Ramanujam, Phys. Rev. A **26**, 3672 (1982); L. J. Curtis (private communication).
[18]Y.-K. Kim and K.-N. Huang, Phys. Rev. A **26**, 1984 (1982).
[19]K. L. Baluja and C. J. Zeippen, J. Phys. B **21**, 1455 (1988).
[20]H. P. Summers (private communication).
[21]W.-J. Qian and Y.-K. Kim, Bull. Am. Phys. Soc. **33**, 939 (1988); Y.-K. Kim (private communication).
[22]E. Hinnov, A. Ramsey, B. Stratton, S. Cohen, and J. Timberlake, J. Opt. Soc. Am. B **4**, 1293 (1987).
[23]W. R. Johnson, S. A. Blundell, and J. Sapirstein, Phys. Rev. A **37**, 2764 (1988).